Electroacoustic characterization of electrokinetics in concentrated pigment dispersions: 3-Methyl-1-(4-carboxyphenyl)-2-pyrazolin-5-one monomethine oxonol

ARTICLE *in* LANGMUIR · JANUARY 1992

Impact Factor: 4.46 · DOI: 10.1021/la00037a053

1 AUTHOR:

John Texter
Eastern Michigan University
232 PUBLICATIONS **2,219** CITATIONS

Electroacoustic Characterization of Electrokinetics in Concentrated Pigment Dispersions: 3-Methyl-1-(4-carboxyphenyl)-2-pyrazolin-5-one Monomethineoxonol

John Texter

Photographic Research Laboratories, Eastman Kodak Company, Rochester, New York 14650–2109

Received May 13, 1991. In Final Form: August 13, 1991

Aqueous dispersions of the title compound, prepared with and without added surfactant (OMT, sodium oleoylmethyltaurine), have parallelepiped particle morphology. Size distribution and specific surface area determinations, measured by transmission electron microscopy and adsorption of pseudocyanine from solution, indicate average equivalent-sphere diameters of approximately 0.12 μm and specific surface areas of approximately 50 m^2/g. Electrokinetic properties were characterized electroacoustically, using electrokinetic sonic amplitude (ESA) measurements, as a function of pigment volume fraction (ϕ), pH, and surfactant (OMT) adsorption. The ϕ dependence of the ESA is initially linear (for $\phi < 0.02$). Deviations from this linear behavior for $0.05 > \phi > 0.02$ cannot at present be quantitatively accounted for by the theory of Levine and Neale for double layer and volume fraction effects on electrophoretic mobilities in concentrated suspensions. The span of ESA values assumed as pH is varied indicates a surface (carboxyl) pK_a of 5.0, and particle phase physical parameters (size, $\rho = 1.478$ g/cm^3, $\epsilon = 6.8$) suggest a ζ potential of −19.7 mV at (the pK_a) pH 5. Separate (direct) surface acid–base titrations yield a similar pK_a value (5.15) and also indicate that H^+/Na^+ ion exchange occurs to an extent involving 3–6% of the bulk (carboxy and hydroxyl) acid sites. Electrokinetic measurements indicate the monolayer saturation coverage by OMT to be about 5.3×10^{-5} mol/g. This value is in fair agreement (within experimental error) with the monolayer coverage, 6.2×10^{-5} mol/g, obtained by adsorption from solution.

Introduction

The study of electrokinetic properties of dispersed solids has been a focal point for relating surface chemistry to colloidal stability.[1-3] This is particularly the case for systems influenced chiefly by charge stabilization effects of adsorbates. While much of the extant colloid literature on the stabilization of pigment dispersions has to do with pigments stabilized in low-permittivity liquids,[4-6] the stabilization of organic pigments in aqueous dispersions is a commercially important area where both charge and steric stabilization factors are often important.[7] The present study of aqueous dispersions of the title compound, a yellow pigment (Figure 1a), was undertaken to characterize the *intrinsic* surface charge of the pigment as a function of pH and the effects of surfactant adsorption on the dynamic mobility. This particular pigment has found use in photographic technology for the absorption of blue light.[8-11] The *p*-carboxyphenyl and acidic hydroxyl substituents make this pigment one of the first to be reported, which has an intrinsically negative surface charge due to ionized carboxyl groups. Earlier studies of carboxyl group ionization in aqueous dispersions have largely been restricted to latexes, some of which have had intrinsic carboxyl substitution.[12] Other studies include extrinsically induced charging by the adsorption of long chain carboxylic acids[13] on titania[14] and on minerals.[15]

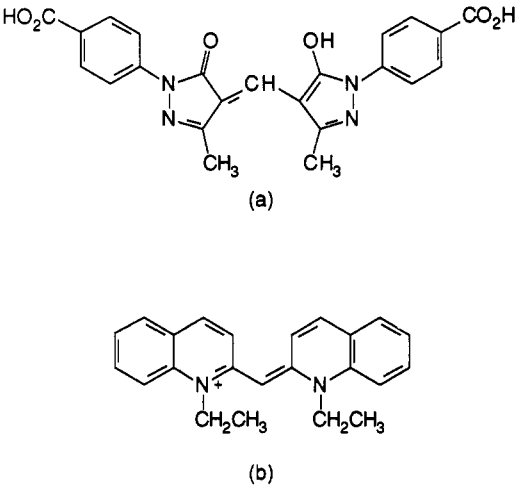

Figure 1. Molecular structures of (a) the title compound, a yellow pigment, 3-methyl-1-(4-carboxyphenyl)-2-pyrazolin-5-one monomethineoxonol {4-[4-[[1-(4-carboxyphenyl)-1,5-dihydro-3-methyl-5-oxo-4H-pyrazol-4-ylidene]methyl]-5-hydroxy-3-methyl-1H-pyrazol-1-yl]-benzoic acid}, and (b) a sensitizing dye (Cy), pseudocyanine {1,1′-diethyl-2,2′-cyanine}, used in relative surface area determinations.

(1) James, R. O.; Parks, G. A. In *Surface and Colloid Science*; Matijavec, E., Ed.; Plenum: New York, 1982; Vol. 12, pp 119–216.
(2) Hunter, R. J. *Foundations of Colloid Science*; Oxford: New York, 1987; Vol. 1, pp 395–449.
(3) Bijsterbosch, B. H. In *Solid/Liquid Dispersions*; Tadros, Th. F., Ed.; Academic: New York, 1987; pp 91–109.
(4) McKay, R. B. *J. Appl. Chem. Biotechnol.* **1976**, *26*, 55.
(5) Ditter, W.; Horn, D. In *Proceedings of the Fourth International Conference on Organic Coatings Science and Technology*; Parfitt, G. D., Patsis, A. V., Eds.; Technomic: Westport, CT, 1978; pp 114–145.
(6) McKay, R. B.; Smith, F. M. In *Dispersion of Powders in Liquids—With Special Reference to Pigments*, 3rd ed.; Parfitt, G. D., Ed.; Applied Science: London, 1981; pp 471–505.
(7) Black, W. In *Dispersion of Powders in Liquids—With Special Reference to Pigments*, 3rd ed. Parfitt, G. D., Ed.; Applied Science: London, 1981; pp 149–201.
(8) Lemahieu, R. G.; Depoorter, H.; Vanassche, J. U.S. Patent 4,092,168, 1978.
(9) Aillet, M. W.; Moelants, F. J.; Mampaey, R. G. U.S. Patent 4,770,984, 1988.
(10) Factor, R. E.; Diehl, D. R. U.S. Patent 4,855,221, 1989.
(11) Schmidt, R. J.; Rocha, H. P. U.S. Patent 4,904,565, 1990.
(12) Ottewill, R. H.; Shaw, J. N. *J. Electroanal. Chem. Interfacial Electrochem.* **1972**, *37*, 133.
(13) Hunter, R. J. *Zeta Potential in Colloid Science—Principles and Applications*; Academic: San Diego, CA, 1981; pp 319–321.
(14) Purcell, G.; Sun, S. C. *Trans. Metall. Soc. AIME* **1963**, *226*, 6.

0743-7463/92/2408-0291$03.00/0

The electrokinetic analysis of fine-particle dispersions of organics with sizes on the order of a few tenths of a micrometer and less is complicated in concentrated systems because of the paucity of experimental methods for measuring properties proportional to electrokinetic mobility and dynamic surface charge. The recent introduction of instrumentation to measure colloid vibration potential (CVP, Pen Kem)[16,17] and electrokinetic sonic amplitude (ESA, Matec Applied Sciences)[18-21] has made direct studies of concentrated colloidal dispersions more readily accessible. ESA is the experimental measurement of choice in aqueous slurries of relatively high conductivity, such as those examined in this study, and is the measurement of the ultrasonic pressure (sound) response to an applied radio frequency (rf) field ($f \approx 1$ MHz). The response of such measurements has been derived by O'Brien[22-24] and by Cannon.[20,21] The electrokinetic sonic amplitude (with units of pressure divided by rf-field intensity) can be written[25,26]

$$\mathrm{ESA} = c_c\, \Delta\rho\, \phi\, \mu(\omega)\, G(\omega,\phi) = \gamma S \qquad (1)$$

where c_c is the velocity of sound in the colloidal dispersion, $\Delta\rho$ is the difference of densities of the continuous and discontinuous phases, ϕ is the volume fraction of the particulate phase, $\mu(\omega)$ is the dynamic (electrophoretic) mobility, $G(\omega,\phi)$ is a geometrical and acoustic coupling factor, γ is an instrumental (cell) constant determined by calibration, and S is the signal (with units of ESA) measured by the instrumentation. O'Brien[23] has shown for parallel-plate geometry with rigid walls (plates, no acoustic coupling out of the cell), that $G(\omega,\phi)$ is given by the expression

$$G(\omega,\phi) = \{1 - \cos(\omega L/c_c)\}/\sin(\omega L/c_c) \qquad (2)$$

where ω is the angular frequency of the rf-field and L is the separation between the plates. In practice the cell walls are not perfectly rigid, and there is acoustic coupling out of the cell. Cannon[20,21] has derived an expression for $G(\omega,\phi)$ that accounts for the acoustic coupling in a parallel-plate cell of the structure illustrated in Figure 2. This expression for $G(\omega,\phi)$ is given as

$$G(\omega,\phi) = Z_r/\{Z_c + \omega M \cot(kL) - iZ_r \cot(kL)\} \qquad (3)$$

where $Z_r = \rho_r c_r$ is the acoustic impedance of the buffer rod connecting the sample cell and the piezoelectric transducer, $Z_c = \rho_c c_c$ is the acoustic impedance of the colloid suspension, ρ_r and ρ_c are the respective average densities, k is the wavevector for sound propagation in the suspension, M is the mass per unit area of the electrode, and

$$k = \omega\chi^{1/2}/(1 + i\,\phi\,\Delta\rho/\rho_c)^{1/2} \qquad (4)$$

where χ is the bulk compressibility of the colloidal dispersion. In other geometries $G(\omega,\phi)$ must be determined as part of an effective cell constant, $\gamma/G(\omega,\phi)$,[26] determined by calibration.

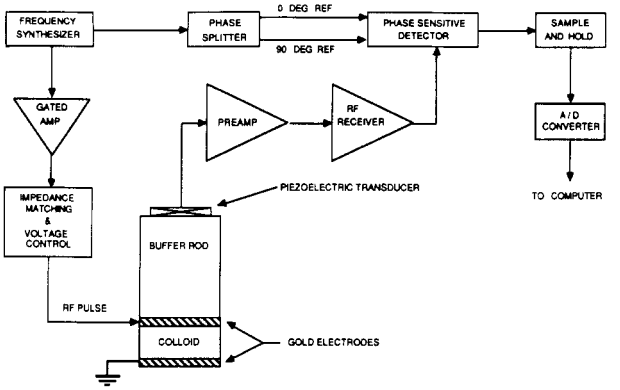

Figure 2. Block diagram of MBS 8000 electrokinetic sonic amplitude measurement system. (Courtesy of D. W. Cannon and L. C. Lynnworth and reproduced by permission of Academic Press, Inc., from Figure 9-18 in ref 19.)

According to eq 1, after suitable calibration, ESA measurements permit a direct estimation of the dynamic mobility, $\mu(\omega)$. This *dynamic* mobility may be used to determine the *static* mobility, $\mu(0)$.[22,24,25] This static electrophoretic mobility, electrolyte, and other conditions can then be used to calculate zeta potential and surface charge density.[27,28]

Experimental Section

Materials. The yellow pigment was obtained from Dr. Donald Diehl of the Photographic Research Laboratories, Eastman Kodak Co., and the surfactant, OMT (sodium oleoylmethyltaurine), was obtained from Mr. John Bishop of the Emulsion Processing Division, Eastman Kodak Co. The pseudocyanine (Cy) sensitizing dye (tosyl salt), used in dye adsorption isotherms, was obtained from Ms. Freddye Price of the Photographic Research Laboratories, Eastman Kodak Co. The structures of this pigment and the pseudocyanine are illustrated in Figure 1. High-purity sodium dodecyl sulfate (SDS), used as a titrant standard in surfactant adsorption isotherm assays, and dimidium bromide/disulfine blue VN indicator solutions used in the same assays were obtained from BDH Chemicals. Cetyltrimethylammonium bromide (CTAB), used as titrant in surfactant assays, was obtained from Kodak Laboratory and Research Products.

Dispersion Preparation. Aqueous dispersions of the pigment *without added surfactant* were prepared by standard roller-milling techniques.[29] ZrO_2 media 1.8 mm in diameter were utilized at a charge ratio of approximately 50-53%. Dispersion A (approximately 450 g) was prepared at a level of 10% pigment by weight and milled in a 1-qt jar at 50% of critical speed for 7 days. Dispersion B (2 kg) was prepared at a level of 7% pigment (by weight) and milled in a 1-gallon jar for 10 days at 40% of critical speed.

Particle Sizing. Transmission electron micrographs were prepared by diluting the dispersions, spotting sample grids with dilute slurry, and, after drying, shadowing the grids with Pt/Pd to allow particle thickness to be estimated. Size distributions were generated by measuring equivalent lengths, heights, and widths of individual particles (equivalent in the sense that each particle was approximated as a parallelepiped). Equivalent particle heights were obtained by measuring the shadow length and correcting for the shadowing angle determined by the location

(15) Park, A. S.; Raby, L. H.; Wadsworth, M. E. *Soc. Min. Eng., Trans.* **1966**, Sept, 301.
(16) Marlow, B. J.; Fairhurst, D.; Pendse, H. P. *Langmuir* **1988**, *4*, 611.
(17) Marlow, B. J.; Rowell, R. L. *Energy Fuels* **1988**, *2*, 125.
(18) Oja, T.; Peterson, G. L.; Cannon, D. W. *U.S. Patent 4,497,201*, 1985.
(19) Lynnworth, L. C. *Ultrasonic Measurements for Process Control*; Academic: New York, 1989; pp 579-586.
(20) Cannon, D. W. In *International Symposium on Surface Charge Characterization, San Diego, CA, August 1990*; Oka, K., Ed.; Fine Particle Society: Tulsa, OK, 1990; Supplement.
(21) Cannon, D. W. To be submitted for publication in *Rev. Sci. Instrum.*
(22) O'Brien, R. W. *J. Fluid Mech.* **1988**, *190*, 71.
(23) O'Brien, R. W. *J. Fluid Mech.* **1990**, *212*, 81.
(24) O'Brien, R. W.; Midmore, B. R.; Lamb, A.; Hunter, R. J. *Discuss. Faraday Soc.* **1990**, *90*, 301-312.
(25) James, R. O.; Texter, J.; Scales, P. J. *Langmuir* **1991**, *7*, 1993.
(26) Klingbiel, R. T.; Coll, H.; James, R. O.; Texter, J. *Part. Sci. Technol.*, submitted for publication.
(27) White, L. R.; Mangelsdorf, C. S.; Chan, D. Y. C. *Mobility User Manuel*; Department of Mathematics, University of Melbourne: Melbourne, 1989.
(28) O'Brien, R. W.; White, L. R. *J. Chem. Soc., Faraday Trans. 2* **1978**, *74*, 1607.
(29) Wheeler, D. A. In *Dispersions of Powders in Liquids—With Special Reference to Pigments*, 3rd ed.; Parfitt, G. D., Ed.; Applied Science: London, 1981; pp 327-361.

of the Pt/Pd source relative to the sample grid. These detailed dimensional data, along with the pigment density, were used to numerically generate equivalent-sphere number-frequency distributions. Pigment density was determined by CsCl density centrifugation of dispersion samples. Centrifuge samples were prepared by adding 25 μL of dispersion to a heat-sealable tube that was then filled with 39% (w/w) CsCl solution. The tubes were sealed and spun for 18 h at 60 000 rpm, generating a gradient ranging from 1.2 to 1.6 g/cm^3. The tube contents were then pumped through a spectrophotometer and a mass density meter, and densities were assigned from strip chart recordings.

Adsorption Isotherms. Adsorption from solution was determined by incubating dispersion samples with adsorbate (dye or surfactant) while stirring, separating the pigment from the continuous phase by high-speed centrifugation (Du Pont Sorvall RCB-1000), and analyzing the supernatant for remaining adsorbate. Adsorption isotherms of the pseudocyanine (Cy) were measured at 25 °C and pH 5.05 using a Teorell and Stenhagen universal buffer[30] (phosphate/citrate/borate) at an ionic strength of approximately 0.05 M. Test slurries (100 mL) were prepared with approximately 6.1 mg of pigment and 0–0.5 μmol of Cy. Since the pseudocyanine undergoes a reversible proton addition[31] (with concomitant decoloration) with pK_a of 4.0,[32] aliquots of supernatant were adjusted to pH 7 for absorption measurements at the λ_{max} (522 nm, ϵ = 65 900 ± 300 (L/mol)/cm). Similarly, adsorption isotherms of the surfactant OMT were made by analyzing aliquots of supernatant for OMT using a two-phase colorimetric titration method.[33,34] The OMT adsorption isotherms were done using the same buffer system described above at pH 5.05. Test slurries, 55–80 mL in volume, contained 2 g of pigment and 50–300 μmol of OMT. The OMT assays were run using CTAB (standardized against high purity SDS) as titrant. Pigment weight (volume) concentrations ranged from 2.5% (1.7%) to 3.6% (2.5%).

Electrokinetic Measurements. Electrokinetic sonic amplitude measurements were made using a Matec electrokinetic sonic analysis system, essentially configured as described by Babchin et al.[35] and by Lynnworth.[19] A block diagram of the instrumentation is shown in Figure 2. The Matec MBS-8000 amplifier rack was controlled by the Matec software STESA in the single-point mode, and utilized a WYSE 286 computer, a Wavetek Model 23 signal generator, an Iwatsu Model SS-5710 oscilloscope, and a Matec SP-80 rf/ultrasonic transducer. This transducer, illustrated schematically in Figure 2, consists of a piezoelectric transducer affixed to the end of an acoustic buffer rod. A gold-plated disk electrode, approximately 25 mm in diameter, is attached to the other end of the acoustic buffer rod. This electrode and associated bonding material also serve as an acoustic interface between the colloidal dispersion and the buffer rod. An opposing electrode, consisting of a 1.4 mm × 3 mm × 40 mm (gold plated) bar, was symmetrically fixed opposite the disk electrode (1.4 mm × 40 mm surface parallel to disk electrode) at a separation of approximately 1.5 mm. The rf-field frequency (cf. eqs 2–4) was tuned to maximize the ESA response in the test slurries. Measurements were typically made in 150-mL beakers at 25 °C with stirring on test slurries typically 100 mL in volume. Measurements were periodically repeated after ultrasonicating the test slurry to ensure that slow flocculation effects were not affecting the measurements. The measurement of ESA magnitude was calibrated[25,26,36] using colloidal silica (Ludox TM, Du Pont) at a 10% (v/v) concentration (ESA/$G(\omega,\phi)$ = −5.21 mPa·m/V for $\omega \approx 2\pi \times 10^6$ rad/s and ϕ = 0.1). This same standard was used to set the relative phase. This ESA/$G(\omega,\phi)$ value of −5.21 mPa·m/V used for calibration differs substantially from the −3.67 mPa·m/V value suggested by the manufacturer, but was derived experimentally from detailed studies of colloidal silica, polystyrene and poly(methyl methacrylate) latexes, and colloidal alumina.[25,26]

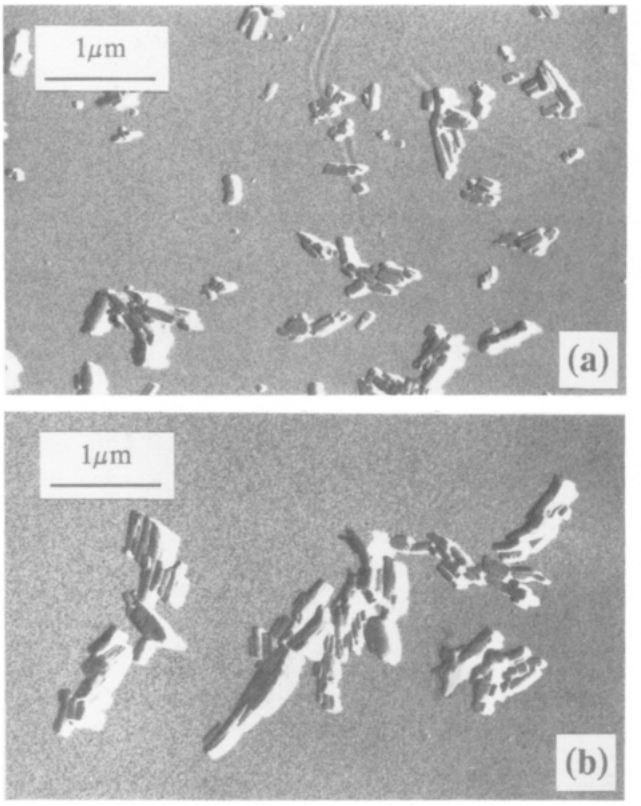

Figure 3. Transmission electron micrographs of pigment dispersions (a) A and (b) B. Shadows were created by Pt/Pd sputtering.

Dielectric Constant. The dielectric permittivity of the pigment was determined over the range of 0.9–2.0 MHz by measuring the permittivities of a series of suspensions of pigment in paraffin wax. Pigment (powder) was added to melted wax, and the slurry was then sonicated to effect dispersion. Coatings of the melted suspensions were made on aluminum foil. Punches (4.866 cm^2) of the coatings were placed in the sample holder and the capacitance at room temperature was measured using a Hewlett-Packard HP-109A admittance meter. After removal from the sample holder, coating thicknesses were measured with a micrometer.

Surface Titrations. Titrations of pigment slurries were made potentiometrically using a Radiometer Copenhagen REC80/TTT80 titration system. Samples of dispersion at a volume fraction of 0.026 in 0.04 M NaCl at 25 °C and initial pH of 5.2 were preequilibrated at pH 3 by potentiostatic addition of 0.2 M HCl. Slurries were then titrated with 0.1 M NaOH.

Results and Discussion

Particle Size Distributions and Specific Surface Areas. The predominant morphology is that of parallelepipeds, as illustrated in Figure 3 for dispersions A and B. The primary flow particles[37] appear to be small agglomerates (less than 1 μm in largest dimension). Analysis of the shadow lengths indicated that the smallest dimension generally was the thickness; volume-weighted averages were 0.082 and 0.107 μm, respectively, for A and B (derived from size distribution data). Several micrographs of each of these dispersions were analyzed, and x, y, and z dimensions of individual particles were tabulated

(30) Perrin, D. D.; Dempsey, B. *Buffers for pH and Metal Ion Control*; Chapman and Hall: New York, 1974; pp 38, 54.
(31) Scheibe, G. *Chimia* **1961**, *15*, 10.
(32) Herz, A. H. *Photogr. Sci. Eng.* **1974**, *18*, 207.
(33) Reid, V. V.; Longman, G. F.; Heinerth, E. *Tenside* **1967**, *4*, 292.
(34) Heinerth, E. In *Anionic Surfactants—Chemical Analysis*; Cross, J., Ed.; *Surfactant Science Series*; Marcel Dekker, New York, 1977; Vol. 8, pp 221–233.
(35) Babchin, A. J.; Chow, R. S.; Sawatzky, R. P. *Adv. Colloid Interface Sci.* **1989**, *30*, 111.
(36) Klingbiel, R. T.; Coll, H.; James, R. O.; Texter, J. In *International Symposium on Surface Charge Characterization, San Diego, CA, August 1990*; Oka, K., Ed.; Fine Particle Society: Tulsa, OK, 1990; pp 20–21.
(37) Lawrence, S. In *Dispersion of Powders in Liquids—With Special Reference to Pigments*, 3rd ed. Parfitt, G. D., Applied Science: London, 1981; pp 363–394.

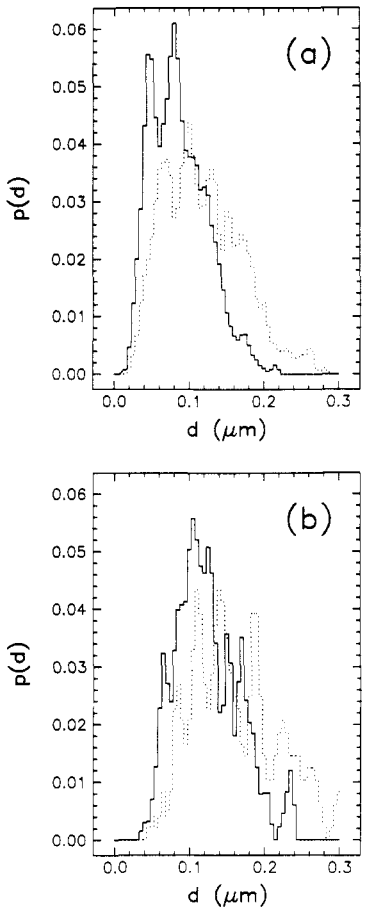

Figure 4. Normalized equivalent-sphere, $p_v(d)$ (···), and volume-weighted, equivalent(surface area-to-volume)-sphere, $p_\varphi(d)$(——), particle-size distributions for pigment dispersions (a) A and (b) B.

so that number frequency particle-size distributions could be calculated. Two types of normalized distributions are illustrated in Figure 4 for both dispersions A and B. The $p_v(d)$ are equivalent-sphere distributions; the volume of each particle was converted to an equivalent spherical diameter in constructing the illustrated histograms. The $p_\varphi(d)$ distributions are equivalent(surface-to-volume)-sphere distributions; the surface-area-to-volume ratio of each particle was converted to an equivalent spherical diameter having the same surface area-to-volume ratio; the number frequency was weighted by the number of such equivalent spherical volumes contained in the actual particle. Analysis of the (raw) equivalent-parallelepiped x, y, and z data for each particle, and a measured density of 1.478 (±0.008) g/cm^3 (determined by CsCl density gradient centrifugation), yielded specific surface areas of 54 and 48 m^2/g, respectively, for dispersions A and B.

The mode maxima of the $p_\varphi(d)$ distributions correspond to the respective volume-weighted thicknesses 0.082 and 0.107 μm. The specific surface areas derived for the respective dispersions correspond to monodisperse spherical diameters of 0.111 and 0.124 μm. These equivalent diameters correspond to the approximate mode maxima in the respective $p_v(d)$ distributions.

Relative specific surface areas were also examined by measuring the saturation (monolayer) adsorption of the pseudocyanine dye (Cy, Figure 1b). Adsorption from solution was done at pH 5.05 (buffered) and 25 °C where the buffer was approximately 0.05 M in ionic strength. Typical results are illustrated in Figure 5 for dispersion A. The adsorption is accurately modeled by the Langmuir adsorption equation.[38] Monolayer coverages, η_s, of 4.08 (±0.11) × 10^{-5} and 3.29 (±0.56) × 10^{-5} mol/g (dye/pigment) and binding constants of $10^{6.0\pm0.3}$ and $10^{6.0\pm0.2}$ L/mol were obtained for dispersions A and B, respectively. The monolayer coverages correspond to adsorbed dye areas of 221 and 242 Å^2/molecule, respectively, for dispersions A and B, when the specific surface areas determined from the transmission electron micrographs are taken into account. These results indicate an average area per adsorbed dye molecule of 232 Å^2 (±6.4%) at saturation. This area is 4 times larger than that obtained in (close-packed) J-aggregate adsorption of pseudocyanine on AgBr surfaces (58.0 ± 0.3 Å^2/molecule).[39-41] We can therefore conclude that Cy adsorption in this system does not involve significant aggregation, since the area per molecule is so much larger than that observed in J-aggregates. Application of this Cy adsorption method to other pigments should be accompanied by other independent measures of surface area (such as image analysis of transmission electron micrographs in this report). At present, it is not possible to ascertain how the Cy molecule attaches to the pigment surface. Interactions between the ammonium nitrogen and (ionized) pigment carboxyl groups are likely candidates for the driving force of interaction. Van der Waals interactions between the π systems of the pigment and Cy molecules may also be primary components of the driving force for Cy adsorption in this system.

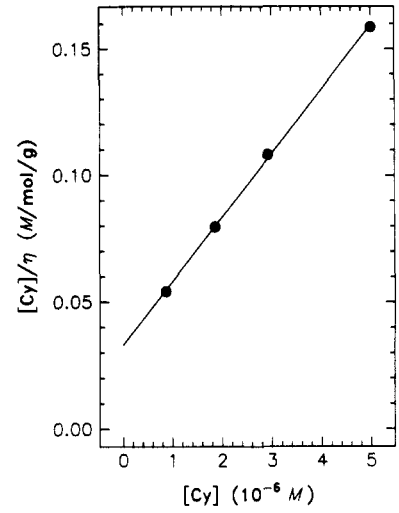

Figure 5. Adsorption isotherm of pseudocyanine dye (Cy) in dispersion A at 25 °C in 0.05 M ionic strength buffer at pH 5.05. The monolayer coverage η_S = 3.96 × 10^{-5} mol/g (dye/pigment) and the binding constant is $10^{5.88}$ L/mol.

Volume Fraction Dependence of the ESA Signal. The volume fraction variation of the ESA/G magnitude obtained for dispersion A is illustrated in Figure 6. These data are means and standard deviations of repeat determinations. The test samples were maintained at 25 °C with continuous phases 0.01 M in $NaNO_3$ and pH 5.8 ± 0.1. Successive data points were obtained by diluting the test slurries with 0.01 M $NaNO_3$. The variation of ESA/G magnitude with volume fraction is linear for ϕ <0.02 (3% (w/w)). A linear least-squares fit to the data for ϕ < 0.02 indicates a slope, d(ESA/G)/dϕ, of −18.34 ± 0.28 mPa·m/V. The corresponding 99% confidence interval for this slope is −19.46 to −17.23 mPa·m/V. According to eq 1 with c_c = 1480 m/s and $\Delta\rho$ = 0.481 (±0.008) g/cm^3, a

(38) Adamson, A. W. *Physical Chemistry of Surfaces*, 2nd ed.; Interscience: New York, 1967; pp 398-402.
(39) Herz, A. H. *Adv. Colloid Interface Sci.* **1977**, *8*, 237.
(40) Gunther, E.; Moisar, E. *J. Photogr. Sci.* **1965**, *13*, 280.
(41) Herz, A. H.; Helling, J. *J. Colloid Interface Sci.*, **1966**, *22*, 391.

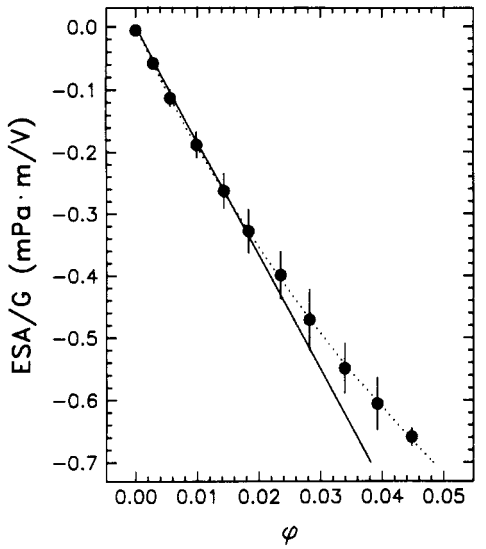

Figure 6. Variation of electrokinetic sonic amplitude (ESA) as a function of pigment volume fraction, ϕ, at 25 °C with a continuous phase 0.01 M in $NaNO_3$. The straight line illustrates a linear fit to the data with $\phi < 0.02$ (3% (w/w)) and illustrates that deviations from the first-order theory occur above this volume fraction; the slope of this line is −18.34 ± 0.28 mPa·m/V. The dotted line is a fit of the data to the function $\alpha\phi(1-\phi)/(1+\beta\phi)$ with parameters −20.76 ± 0.27 mPa·m/V and 7.52 ± 0.48 for α and β, respectively.

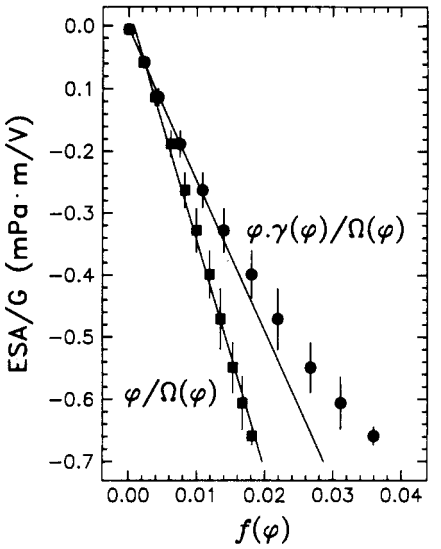

Figure 7. Variation of electrokinetic sonic amplitude (ESA) as a function of $f(\phi)$ for two cases at 25 °C with a continuous phase 0.01 M in $NaNO_3$. These are the same data as plotted in Figure 6. In case 1, with $f(\phi) = \phi\gamma(\phi)/\Omega(\phi)$ (the sedimentation potential correction), no improvement in accounting for deviation from linearity with increasing volume fraction (Figure 6) is obtained. In case 2, with $f(\phi) = \phi/\Omega(\phi)$, the volume fraction dependence of the ESA is accounted for (empirically).

dynamic mobility, $\mu(\omega)$, of −2.58 ± 0.08 μm·cm/(s·V) is obtained at this pH of 5.8 and $\omega = 2\pi \times 10^6$ rad/s.

The deviation from linearity in ϕ, illustrated in Figure 6, can arise from hydrodynamic and electrical particle–particle interactions and from acoustic coupling effects. Levine and Neale[42] have derived, using the Kuwabara cell model[43] for hydrodynamic interactions, an analytical extension of Henry's theory[44,45] for the κa and volume fraction dependence of electrophoretic mobilities. Levine and Neale showed that this variation can be expressed as a function $f(\kappa a, \phi) \in (0,1)$, which is introduced as a multiplier in eq 1 to give

$$\mathrm{ESA} = c\,\Delta\rho\,\phi\,\mu(\omega)\,f(\kappa a,\phi)\,G(\omega,\phi) \qquad (5)$$

At the electrolyte levels used in this study, 0.01–0.05 M, κa varies from 40 to 90. The double layer is fairly compressed at these concentrations, and the function $f(\kappa a,\phi) \approx 0.95$ for $\phi < 0.1$. This theory predicts therefore that ESA/G is a *linear function of volume fraction* in compressed double layer systems. The experimental data illustrated in Figure 6 indicate that this theory is not applicable to the present system for $\phi > 0.02$. While Reed and Morrison[46] have shown that electrophoretic mobilities in dilute systems (where particles do not interact) are independent of particle shape, and the primary particles in this study are parallelepipeds rather than the spheres examined by Levine and Neale, the primary *flow* particles in this study *may* be small aggregates (cf. Figure 3). The aggregation illustrated in Figure 3 may be an artificat of speciman preparation, although long-time (gravitational) sedimentation of these dispersions strongly suggests that the primary flow particles *are* aggregates. Hence, although the double layer is compressed, particles in clusters *do interact strongly*, and the derivation of Levine and Neale does not include electrical interactions other than diffuse double layer repulsion.

In an exposition of the colloid vibration potential (CVP) of concentrated titania suspensions, Marlow et al.[16] invoked a Kuwabara-cell-model-based theory of Levine and co-workers[47] to account for ϕ variations in the CVP. This theory of Levine, Neale, and Epstein was developed to account for the double layer thickness and volume fraction dependence of *sedimentation* potentials in concentrated systems. While it is not entirely clear when electrophoretic mobility can be equated to gravitational or centrifugal mobilities, electrophoretic mobility is the kernel of both CVP and ESA phenomena, and the treatment of Levine and Neale[42] showed that electrical and hydrodynamic interactions result in a volume fraction independence of the electrophoretic mobility in systems with fully compressed double layers. Marlow et al.[16] introduced the (sedimentation potential based) correction factor

$$\gamma(\kappa a,\phi)/\Omega(\phi) \approx (1+23\phi)(5-9\phi^{1/3}+5\phi-\phi^2)/5 \qquad (6)$$

where the function $\gamma(\kappa a,\phi) \to \gamma(\phi)$ as $\kappa a \to \infty$ and $\gamma(\phi) \approx (1+23\phi)$ for $\phi < 0.2$. Marlow et al. indicated that this function can be approximated by the form $1-\phi$, for $\kappa a \gg 1$, and explained qualitatively in terms (introduced by Zukowski and Saville[48,49]) of the back-flow of continuous phase into void volume created by particle movement. Marlow et al. found that this sedimentation potential-based correction gave quantitative agreement with experiment in the case of a colloidal alumina-clad titania suspension (R-100, Du Pont) over a volume fraction range $0 < \phi < 0.35$.[16] The application of this correction is illustrated in Figure 7, where the experimental ESA/G data are plotted as functions of volume fraction correction functions, $f(\phi)$. In the case where $f(\phi)$ is equated to the

(42) Levine, S.; Neale, G. *J. Colloid Interface Sci.* **1974**, *47*, 520.
(43) Kuwabara, S. *J. Phys. Soc. Jpn* **1959**, *14*, 527.
(44) Henry, D. C. *Proc. R. Soc. London, A* **1931**, *133*, 106.
(45) Henry, D. C. *Trans. Faraday Soc.* **1948**, *44*, 1021.
(46) Reed, L. D.; Morrison, F. A., Jr. *J. Colloid Interface Sci.* **1976**, *54*, 117.
(47) Levine, S.; Neale, G.; Epstein, N. *J. Colloid Interface Sci.* **1976**, *57*, 424.
(48) Zukowski, C. F.; Saville, D. A. *J. Colloid Interface Sci.* **1987**, *115*, 422.
(49) Zukowski, C. F. Studies of Electrokinetic Phenomena in Suspensions, Thesis, Princeton University, 1985; pp 247–287.

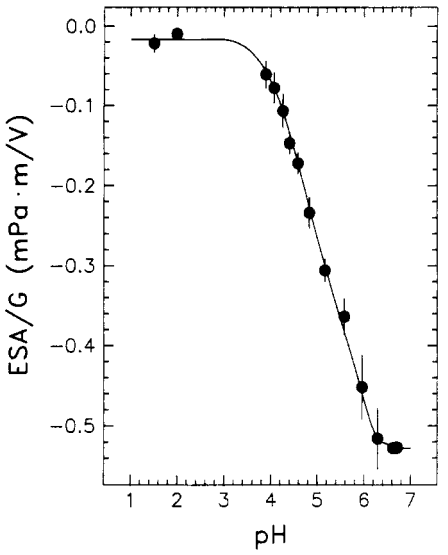

Figure 8. Variation of ESA as a function of pH at 25 °C for a dispersion slurry with $\phi = 0.024$ in $I = 0.05$ M phosphate/citrate/borate buffers. The apparent surface pK_a is approximately 5.0.

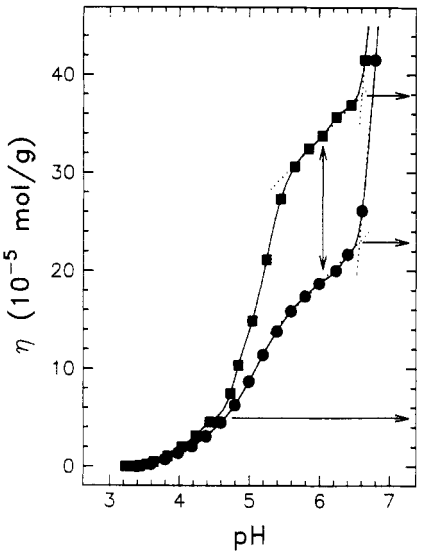

Figure 9. Potentiometric titration of pigment "surface" acidity at 25 °C for slurries of dispersion A with (initially) $\phi = 0.026$ in 0.04 M NaCl; preequilibrated 2 h (●) and 16 h (■) potentiostatically at pH 3 with 0.1 M HCl. After preequilibration, titrations were done with 0.1 M NaOH. The uptake η is expressed in terms of moles of hydroxide per grams of pigment. Break points are indicated by the horizontal arrows at successive η of 5×10^{-5}, 23×10^{-5}, and 38×10^{-5} mol/g.

$\phi\gamma(\phi)/\Omega(\phi)$ form derived from eq 6, this correction gives no improvement whatever in accounting for the deviation illustrated in Figure 6. It is noteworthy, however, that the other correction factor plotted in Figure 7, $f(\phi) = \phi/\Omega(\phi)$, *does* result in an empirical accounting of the deviation illustrated in Figure 6. The function $\phi/\Omega(\phi)$ may be approximated by a function of the form $\phi(1-\phi)/(1+\beta\phi)$. Such forms were introduced empirically by Zukowski and Saville to account for conductivity variations with ϕ in concentrated suspensions of red blood cell ghosts. A least-squares fit of the ESA/G data to the function $\alpha\phi(1-\phi)/(1+\beta\phi)$ yields parameters −20.76 ± 0.27 mPa·m/V and 7.52 ± 0.48 for α and β, respectively.

Surface Charge and Mobility as a Function of pH. Electrokinetic charge variation with pH is illustrated in Figure 8 for a series of slurries (dispersion A) prepared in phosphate/citrate/borate buffers (I = 0.05 M). The pigment was present at a volume fraction of 0.024. Dissolution of pigment begins to become significant at pH > 6.5. An apparent pK_a of 5.0 is indicated as the midpoint of the domain of ESA/G. The negative charge density is due to ionized surface carboxyl groups, and essentially disappears as the pH is lowered. There are no basic surface groups that add protons; hence there is no (crossover) point of zero charge for pH > 0.

An alternative approach to investigating the effects of pH on surface ionization is to directly titrate the surface acid groups potentiometrically. Data obtained in two such experiments are illustrated in Figure 9 and expressed in terms of integral hydroxide uptake, η (mol of OH^-/g of pigment). The variation illustrated at pH > 6.5 arises as a result of pigment *dissolution*. The illustrated titrations were done with 0.04 M NaCl as supporting electrolyte. The initially prepared slurries contained 4 g of pigment at a volume fraction of 0.025 and were 5.1–5.2 in pH. The slurries were first potentiostatically adjusted to pH 3 with 0.1 M HCl, and then titrated with 0.1 M NaOH. The two illustrated titration curves differ in the length of time the slurries were preequilibrated at pH 3 (2 and 16 h). This preequilibration involved a slow but substantial uptake of protons. The amounts of acid taken up by the slurries in reducing the pH to 3 in the two cases were 18×10^{-5} and 33×10^{-5} mol/g, respectively, for the 2 and 16 h preequilibrations. It is noteworthy that these preequilibrations correspond on a mole of hydroxide per mole of pigment basis to uptake fractions of 0.080 and 0.146 mol/mol, respectively. Since the pigment is a triprotic acid, these uptakes correspond to 2.7% and 4.9%, respectively, of the total acid functionality. The shape of the uptake–pH curves indicates two classes of ionizable groups. One class is characterized by behavior illustrated over the pH range of 3.0–4.6, and the second class is characterized by a significantly greater transition over the 4.6–5.6 pH range. The *pre*dissolution limits on η, obtained from respective break points, are 23×10^{-5} and 38×10^{-5} mol/g, respectively, for the 2 and 16 h preequilibrations. These overall limits on hydroxide uptake indicate for both curves that the effective pK_a is 5.15, in fair agreement with the electroacoustic result of 5.0 illustrated in Figure 7. Over the pH range of 5.6–6.6, the two titration curves differ in η by a constant 15×10^{-5} mol/g, which is precisely the difference in preequilibration acid uptake between the two experimental runs. The magnitude of this effect suggests that significant *bulk* ion exchange (H^+/Na^+) occurs in addition to surface ionization. However, it is difficult to say how this exchange is distributed throughout the material. The volume weighted average particle thickness for dispersion A was found earlier to be 820 Å. If we presume, based on molecular space-filling models, that the pigment packs as a parallelepiped isomorphically with the particle, approximately 160–215 molecules span the thickness of the average particle. The ion exchange that occurs may very well be *concentrated* toward the particle periphery. The *pre*dissolution uptakes of 23×10^{-5} and 38×10^{-5} mol/g correspond respectively to 39.0 and 23.6 Å^2/acid site, if it is assumed that all ionization occurs on the surface. Since the molecular volume is 500 Å^3/molecule, we can estimate the average surface area per molecule to be about 100 (±30) Å^2, assuming the pigment molecule is 4–5 Å thick. This estimate and the 39.0 and 23.6 Å^2/acid site limits indicate that all of the surface molecules are triply ionized. If that were the case, all of the surface molecules would be present as a trisodium salt phase. A more realistic estimate of the extent of surface ionization is obtained from the initial hydroxide uptake below pH 5. A break point in both curves of Figure 9 at pH 4.6 suggests an

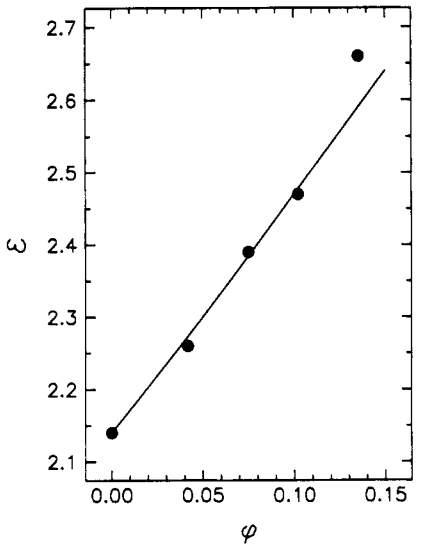

Figure 10. Relative permittivity as a function of pigment volume fraction (ϕ) for pigment–paraffin wax mixtures at room temperature. The curve connecting the data was calculated from fits of the data to two separate models of heterogeneous dielectrics (rods and spheres, eqs 3.108 and 3.93, respectively, in ref 50).

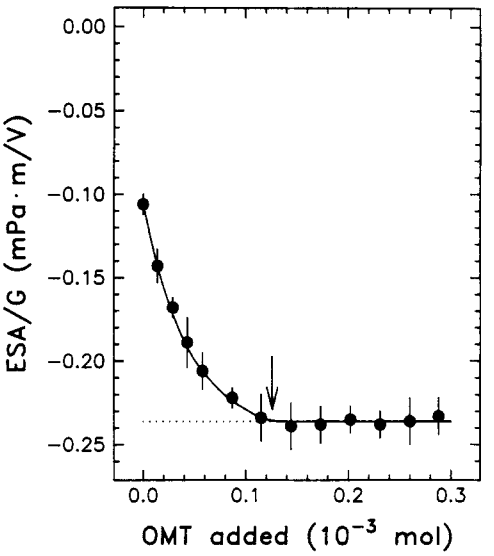

Figure 11. Variation of ESA as a function of added OMT at 25 °C for a (dispersion B) slurry with $\phi = 0.0135$ in pH 5.05 buffer ($I \approx 0.05$ M). The breakpoint at 0.12 mmol added OMT corresponds to 5.3×10^{-5} mol/g (OMT/pigment).

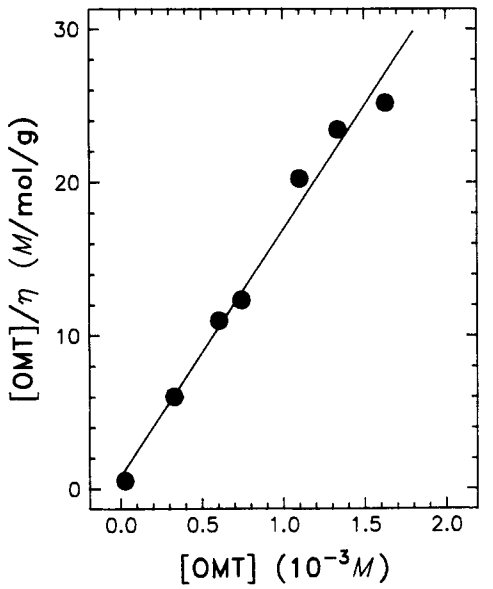

Figure 12. Adsorption isotherm of OMT on pigment at 25 °C for (dispersion B) slurries with $\phi = 0.017$ to 0.025 in pH 5.05 buffer ($I \approx 0.05$ M). The monolayer coverage $\eta_s = 6.23 \times 10^{-6}$ mol/g corresponds to an area of 128 Å²/OMT. The binding constant (Langmuir equation) $b = 10^{4.3}$ L/mol.

initial hydroxide uptake limit of 5×10^{-5} mol/g. This limit corresponds to an area of 180 Å²/surface site and an apparent pK_a of 4.2. The two-component nature of this ionization appears to consist of surface and bulk components. It is therefore not possible to determine the surface charge density directly, since the location and character of the Stern layer cannot be defined with any certainty. The ESA technique, sensitive only to apparent (dynamic) electrokinetic surface charge (as integrated to the hydrodynamic surface of shear), is not sensitive to the (internal) ion-exchange process that occurs at pH < 4.6.

The conversion of ESA/G values to dynamic mobilities, and ultimately zeta potentials, requires some detailed knowledge of the properties of the dispersed phase, such as particle size, dielectric constant, and density.[22] For our present purpose the equivalent spherical diameter of 0.12 μm will be taken as an approximate characterization of particle size. The relative permittivity was determined (to be invariant over the range of 900–2000 kHz) at room temperature by diluting powdered pigment in paraffin wax and fitting the effective dielectric constant data to models for two-phase composite dielectrics. Dielectric loss was found to be negligible over the range of 1–2000 kHz. Under such conditions it is not necessary to determine the permittivity at the operating frequency of the ESA measurement, although it was convenient to do so. Volume fractions were calculated using a density of 1.478 for the pigment and a density of 0.962 for the wax. Effective permittivities are illustrated in Figure 10. These data were analyzed in terms of two models[50,51] for heterogeneous dielectrics to deduce the relative permittivity of the pigment phase. One of these models (eq 3.108 in ref 50) was developed for rods and cylinders, and a least-squares fit yielded a constant of 7.04 (±0.64). The other model,[51] developed for spheres (eq 3.93 in ref 50), yielded a constant of 6.81 (±1.27). These analyses yield an average static dielectric constant of 6.9 ± 0.3, and both models yield the same calculated line illustrated in Figure 10. These physical parameters, along with the ESA/G value of −0.26 mPa·m/V at the (pK_a) pH of 5.0 (Figure 8), when substituted into eq 1, yield a dynamic mobility of −1.53 μm·cm/(s·V). These values when substituted into the equation (eq 6.9 in ref 22)

$$\mu(\omega) = (2\epsilon\zeta/3\eta)|[1 + f'(\omega,\epsilon,\epsilon_p)]G'(\omega a^2/\nu)| \qquad (7)$$

where ζ is the zeta potential, ϵ and ϵ_p are the continuous phase and particle relative permittivities, respectively, η is the continuous phase viscosity, f' and G' are complex functions (see eqs 6.6 and 6.10 in ref 22) of their arguments, ω is the applied field frequency, a (0.06 μm) is the effective particle radius, ν is the kinematic viscosity, $|f'| \approx 1/2$, and $|G'| = 0.994$. These parameters yield a calculated ζ potential of −19.7 mV. Conversion of this zeta potential to surface charge density (at the hydrodynamic shear plane)[52]

(50) van Beek, L. K. H. *Prog. Dielectr.* **1967**, *7*, 69.
(51) Looyenga, H. *Physica* **1965**, *31*, 401.
(52) Reference 13, p 29.

$$\sigma_e = (4Ie/\kappa) \sinh (e\zeta/2kT) \quad (8)$$

where $1/\kappa \approx 14$ Å ($I \approx 0.05$ M), indicates a net charge density corresponding to about 1560 Å^2/charge at (pK_a) pH 5.0. Hence the saturation (high pH) density is approximately 730 Å^2/charge. This magnitude suggests that most of the surface charge, determined above by potentiometric titration (23.6–39 Å^2/acid site), is effectively screened by counterions, and is similar in magnitude to (intrinsic) surface carboxyl ionization in polystyrene latexes at $I = 0.05$ M as reported by Ottewill and Shaw.[12]

Surfactant Adsorption. A slurry of dispersion B in pH 5.05 buffer ($I \approx 0.05$ M) and volume fraction 0.0135 was examined (electroacoustically) as aliquots of 1.3 mM OMT were added to the slurry. The ESA response, corrected for volume fraction changes during surfactant addition, is illustrated in Figure 11. An asymptotic limit to electrokinetic charging is clearly indicated at OMT additions greater than 0.122 mmol (5.3×10^{-5} mol/g). It is significant that the magnitude of charging imparted by a monolayer of adsorbed OMT is approximately equal to the intrinsic electrokinetic charge at pH 5.1. The asymptotic ESA/G value of −0.235 mPa·m/V in Figure 11 yields (eq 1) an asymptotic $\mu(\omega)$ of −2.48 μm·cm/(s·V) after substitution for c, $\Delta\rho$, ϕ, and G'. Repeating the zeta-potential and surface charge density calculations detailed above yields a zeta potential of −31.7 mV and a surface charge density corresponding to 940 Å^2/charge.

An adsorption (from solution) isotherm of OMT on the pigment, obtained by phase separation under similar conditions as described above, is illustrated in Figure 12. The binding constant of $10^{4.3}$ is fairly large, indicating essentially irreversible adsorption. The monolayer coverage of 6.23×10^{-5} mol/g corresponds to a surface coverage of 1.3×10^{-10} mol/cm^2, a molecular area of 128 Å^2/OMT, and is in reasonable agreement with the breakpoint illustrated (arrow) in Figure 11 at 0.122 mmol OMT. This monolayer coverage and the charge density estimates described above indicate that at least 86% of the adsorbed surfactant (charge) is compensated by Na^+ inside the hydrodynamic shear plane. Since some of the surface charge density derives from ionized acid groups, this 86% figure is a lower limit.

Acknowledgment. The pigment dispersions were kindly prepared by Mr. Doug Corbin and Mr. Frank Musolino. The transmission electron microscopy was kindly performed by Mr. Anthony Taddei. The CsCl density gradient centrifugation and density measurements were done by Mr. Peter Ghysel. Dielectric constant measurements were made with the kind assistance of Dr. David Jeanmaire. I thank Dr. Robert O. James for useful discussions and for suggestions and corrections given in the preparation of this report.

Registry No. Cy, 14154-05-3; OMT, 137-20-2; 3-methyl-1-(4-carboxyphenyl)-2-pyrazolin-5-one monomethineoronol, 64137-48-0.